Electronic Supplementary Material (ESI) for Sustainable Energy & Fuels.

Hydrogen evolution by polymer photocatalysts; a possible photocatalytic cycle

Andrew W. Prentice and Martijn A. Zwijnenburg*

Department of Chemistry, University College London (UCL), London WC1H 0AJ, United Kingdom

E-mail: m.zwijnenburg@ucl.ac.uk

Supplementary Information

S1 Exploration of Excited States

As mentioned in the main text there is a disagreement between time-dependent density functional theory (TD-DFT) and correlated wave function methods in the ordering of the excited states for small oligomers of poly(*p*-phenylene), PP_n, where n represents the oligomer length. The chemical structure of PP_5 and the Cartesian coordinate system used is shown in Fig. S1, with even and odd oligomer lengths exhibiting D_2 and C_{2h} symmetry, respectively. Fukada and co-workers[1] showed that when using the symmetry-adapted cluster configuration interaction method on PP_2, *in vacuo*, the lowest adiabatic excitation is of 1^1B_3 symmetry, disagreeing with TD-DFT calculations employing the PBE0 functional which instead have the optically bright 1^1B_1 as the lowest energy transition. The gas-phase excited state landscape of PP_2 to PP_8 has also been investigated previously in Ref. 2 using both RI-CC2 and TD-B3LYP. This also showed a disagreement between the ordering of the vertically excited electronic states when using B3LYP and RI-CC2 which was especially apparent for $n = 2, 3$ and 4. For $n \geq 5$ the nature of the lowest vertical transition was in agreement between both methods.

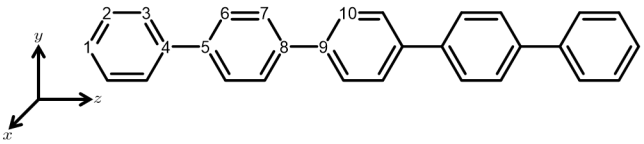

Figure S1: Chemical structure of PP_5 with specific numbering of non-equivalent carbon atoms and the Cartesian coordinate system used.

For each oligomer length of poly(*p*-phenylene) our TD-DFT calcuations predict that the lowest excited state, both in terms of the adiabatic and vertical excitation, is the optically bright state. The vertical transition is described by a single particle-hole transition from the highest occupied to lowest unoccupied molecular orbital, see Table S1 and Table S2 for the adiabatic (AEE) and vertical excited state energies (VEE) of PP_n-H_2O and PP_n-TEA, respectively. For SCS-ADC(2) the VEE of each symmetry is provided in Table S3 and Table S4 for PP_n-H_2O and PP_n-TEA, respectively. The excited state which matches

the ground state symmetry, A and A_g for odd and even oligomer lengths, respectively, has been excluded as it is expected that this state will not be (one of) the lowest energy state(s). In terms of the VEE the picture is somewhat analogous to that in Ref. 2 in which they perform RI-CC2 calculation exclusively *in vacuo*. For PP_2 the 1^1B_2 and 1^1B_3 states are quasi-degenerate, with the optically bright 1^1B_1 state lying at almost 0.6 eV higher in energy. As we increase the oligomer length the bright state drastically lowers in energy when compared to $1^1B_2/1^1B_g$ and $1^1B_3/1^1B_u$ states. For PP_4 the energy spanned by the three states is small at 0.06 eV. For PP_5 and longer chain lengths the optically bright state is the lowest vertical excited state. We then turned out attention to the AEE of each symmetry for SCS-ADC(2). For PP_2-H_2O the lowest SCS-ADC(2) AEE is the 1^1B_3 state (4.588 eV) in agreement with Ref. 1 despite the inclusion of the implicit solvent environment. The higher-lying 1^1B_2 and 1^1B_1 states are located at 4.709 and 4.818 eV, respectively. This disagrees with all DFT calculations which has this as the optically bright state. However, for PP_3 and PP_4 the lowest AEE for ADC(2) corresponds to the optically bright 1^1A_u and 1^1B_1 state, respectively, now in agreement with the density functional theory equivalent calculations. Therefore, for $n \geq 5$ it was sufficient to only optimise the $1^1A_u/1^1B_1$. The AEE for each symmetry for $n = 2, 3$ and 4 and for the bright state for $n \geq 5$ are provided in Table S3. Analogous findings were observed for for SCS-ADC(2) at the PP_n-TEA, see Table S4.

Table S1: The VEE, and corresponding oscillator strength, and the AEE as a function of PP_n-H_2O for each of the exchange-correlation functionals considered. All energies correspond to electronic energies and are provided in terms of eV, with the oscillator strength having arbitrary units.

	B3LYP			CAM-B3LYP			MN15		
PP_n-H_2O	VEE	f	AEE	VEE	f	AEE	VEE	f	AEE
PP_2	4.87	0.57	4.08	5.24	0.56	4.32	5.02	0.59	4.20
PP_3	4.25	1.07	3.49	4.73	1.16	3.84	4.45	1.15	3.67
PP_4	3.92	1.52	3.21	4.47	1.72	3.63	4.16	1.69	3.42
PP_5	3.73	1.92	3.05	4.32	2.28	3.52	3.99	2.21	3.30
PP_6	3.61	2.30	2.96	4.23	2.83	3.48	3.89	2.72	3.23
PP_7	3.53	2.68	2.92	4.17	3.38	3.45	3.82	3.24	3.20

Table S2: The VEE, and corresponding oscillator strength, and the AEE as a function of PP_n-TEA for each of the exchange-correlation functionals considered. All energies correspond to electronic energies and are provided in terms of eV, with the oscillator strength having arbitrary units.

	B3LYP			CAM-B3LYP			MN15		
PP_n-TEA	VEE	f	AEE	VEE	f	AEE	VEE	f	AEE
PP_2	4.87	0.58	4.26	5.25	0.58	4.50	5.03	0.61	4.37
PP_3	4.26	1.09	3.67	4.74	1.17	4.01	4.48	1.15	3.84
PP_4	3.94	1.53	3.37	4.49	1.74	3.78	4.18	1.71	3.58
PP_5	3.75	1.93	3.20	4.34	2.29	3.66	4.01	2.22	3.44
PP_6	3.64	2.30	3.10	4.26	2.84	3.60	3.91	2.73	3.36
PP_7	3.56	2.67	3.04	4.20	3.39	3.58	3.85	3.24	3.32

Table S3: The VEE, and corresponding oscillator strength, and the AEE as a function of PP_n-H_2O for each excited state symmetry considered, values obtained using SCS-ADC(2). All energies correspond to electronic energies and are provided in terms of eV, with the oscillator strength having arbitrary units.

	$1^1B_1/1^1A_u$			$1^1B_2/1^1B_g$			$1^1B_3/1^1B_u$		
PP_n-H_2O	VEE	f	AEE	VEE	f	AEE	VEE	f	AEE
PP_2	5.40	0.68	4.71	4.83	0.00	4.82	4.82	0.00	4.59
PP_3	4.85	1.36	4.19	4.79	0.00	4.75	4.63	0.00	4.42
PP_4	4.60	1.94	3.93	4.65	0.00	4.58	4.59	0.00	4.36
PP_5	4.40	2.51	3.80	4.61	0.00		4.54	0.00	
PP_6	4.38	3.13	3.72	4.58	0.00		4.58	0.00	
PP_7	4.28	3.73	3.69				4.55	0.00	

Table S4: The VEE, and corresponding oscillator strength, and the AEE as a function of PP_n-TEA for each excited state symmetry considered, values obtained using SCS-ADC(2). All energies correspond to electronic energies and are provided in terms of eV, with the oscillator strength having arbitrary units.

	$1^1B_1/1^1A_u$			$1^1B_2/1^1B_g$			$1^1B_3/1^1B_u$		
PP_n-TEA	VEE	f	AEE	VEE	f	AEE	VEE	f	AEE
PP_2	5.41	0.69	4.71	4.82	0.00	4.82	4.82	0.00	4.60
PP_3	4.88	1.37	4.20	4.79	0.00	4.75	4.64	0.00	4.43
PP_4	4.65	1.95	3.94	4.65	0.00	4.58	4.61	0.00	4.38
PP_5	4.48	2.52	3.81	4.63	0.00		4.58	0.00	
PP_6	4.41	3.10	3.74	4.58	0.00		4.61	0.00	
PP_7	4.34	3.66	3.71				4.58	0.00	

S2 Generation of Absorption Spectra

The VEE and corresponding oscillator strengths obtained *via* TD-DFT and SCS-ADC(2) computations were then used to transform the stick peak spectra to an absorption spectrum, by simulating the effect of peak broadening. The absorption intensity (I) at each photon energy (E_p) is obtained as a sum of Gaussian functions, see Eq. 1, centred on the excitation energy of the specific state (E_i) and weighted by the corresponding oscillator strength (f_i). A σ value of 0.2 eV was used, corresponding to a full width at half maximum of 0.5 eV. The E_p ranged from 3.00 to 7.00 eV in 0.01 eV steps. The absorption spectra for each oligomer length employing various theoretical methods are provided in Fig. S2. To observe differences in the shape of the spectra, and not solely the height of the absorption peaks, each intensity is divided by the maximum intensity ($I_{max.}$) across all intensities within the range of 3.00 to 7.00 eV, resulting in the normalised intensity (I'), see Eq. 2.

$$I(E_p) = \sum_{i}^{\text{Num. of States}} f_i e \left(\frac{-E_p - E_i}{2\sigma} \right)^2 \tag{1}$$

$$I'(E_p) = \frac{I(E_p)}{I_{max.}} \tag{2}$$

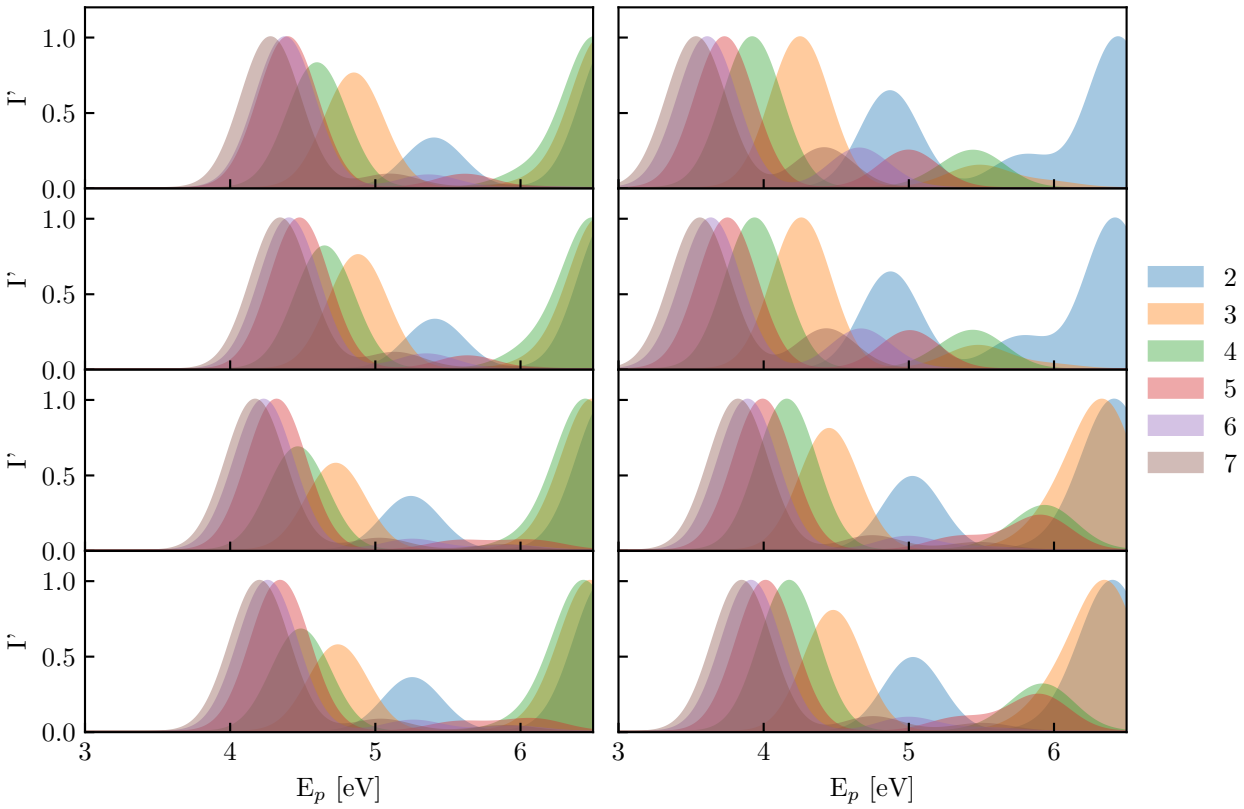

Figure S2: The simulated absorption spectra as a function of PP_n-H_2O (A) and PP_n-TEA (B) calculated using SCS-ADC(2), respectively. The simulated absorption spectra as a function of PP_n-H_2O (C) and PP_n-TEA (D) calculated using TD-CAM-B3LYP, respectively. The simulated absorption spectra as a function of PP_n-H_2O (E) and PP_n-TEA (F) calculated using TD-B3LYP, respectively. The simulated absorption spectra as a function of PP_n-H_2O (G) and PP_n-TEA (H) calculated using TD-MN15, respectively.

S3 Reaction Energetics

Table S5: Various free energy differences of interest within the proposed catalytic cycle, modeled within a water continuum model for each of the exchange correlation functionals. All energy differences are in terms of eV and when applicable pertain to the C_3 hydrogen binding site.

B3LYP														
PP_n-H_2O	Step A	AIP(PP_n)	AEA(PP_n)	AEA(PP_n^*)	AIP(PP_n^*)	AFG	EBE	Step B1	Step B2	Step C1	PT($[TEA\text{-}H]^+$)	Step C2	Step D	H bind.
PP_2	3.93	6.11	1.83	5.76	2.18	4.28	0.35	-0.57	−2.82	−0.76	−0.75	−0.90	−1.26	0.86
PP_3	3.35	5.82	2.09	5.44	2.47	3.74	0.38	-0.25	−2.49	−0.53	−0.51	−0.66	−1.24	0.88
PP_4	3.08	5.69	2.24	5.32	2.61	3.45	0.37	-0.12	−2.37	−0.38	−0.36	−0.51	−1.24	0.88
PP_5	2.92	5.61	2.30	5.22	2.69	3.31	0.39	-0.03	−2.28	−0.32	−0.30	−0.46	−1.24	0.89
PP_6	2.84	5.57	2.34	5.18	2.73	3.23	0.39	0.01	−2.23	−0.27	−0.25	−0.41	−1.25	0.88
PP_7	2.78	5.55	2.37	5.14	2.77	3.19	0.41	0.05	−2.20	−0.24	−0.22	−0.38	−1.25	0.87
CAM-B3LYP														
PP_2	4.18	6.26	1.72	5.90	2.08	4.55	0.36	−0.65	−2.93	−0.92	−0.86	−1.01	−1.21	0.88
PP_3	3.70	6.03	1.93	5.63	2.34	4.10	0.40	−0.38	−2.67	−0.73	−0.66	−0.82	−1.19	0.91
PP_4	3.50	5.92	2.02	5.52	2.42	3.90	0.40	−0.27	−2.56	−0.64	−0.57	−0.73	−1.19	0.91
PP_5	3.40	5.89	2.08	5.48	2.49	3.81	0.41	−0.22	−2.51	−0.59	−0.52	−0.68	−1.19	0.91
PP_6	3.34	5.86	2.10	5.45	2.52	3.76	0.42	−0.20	−2.48	−0.55	−0.49	−0.64	−1.20	0.90
PP_7	3.32	5.84	2.12	5.45	2.51	3.71	0.39	−0.19	−2.48	−0.54	−0.47	−0.62	−1.20	0.90
MN15														
PP_2	4.05	6.26	1.77	5.82	2.21	4.49	0.44	−0.47	−2.91	−0.89	−0.82	−0.82	−1.27	0.81
PP_3	3.53	6.01	2.03	5.56	2.48	3.99	0.45	−0.20	−2.64	−0.63	−0.56	−0.56	−1.27	0.81
PP_4	3.30	5.90	2.18	5.48	2.60	3.72	0.42	−0.13	−2.57	−0.47	−0.41	−0.41	−1.27	0.81
PP_5	3.18	5.85	2.21	5.39	2.67	3.64	0.46	−0.04	−2.47	−0.45	−0.38	−0.38	−1.26	0.81
PP_6	3.11	5.83	2.24	5.35	2.72	3.59	0.48	0.00	−2.43	−0.41	−0.34	−0.34	−1.27	0.80
PP_7	3.08	5.81	2.27	5.35	2.73	3.53	0.45	0.00	−2.44	−0.37	−0.31	−0.31	−1.27	0.80

Table S6: Various free energy differences of interest within the proposed catalytic cycle, modeled within a water continuum model for each of the exchange correlation functionals. All energy differences are in terms of eV and when applicable pertain to the C_3 hydrogen binding site.

B3LYP														
PP_n-TEA	Step A	AIP(PP_n)	AEA(PP_n)	AEA(PP_n^*)	AIP(PP_n^*)	AFG	EBE	Step B1	Step B2	Step C1	PT($[TEA\text{-}H]^+$)	Step C2	Step D	H bind.
PP_2	4.06	6.79	0.98	5.04	2.73	5.81	1.75	1.02	−1.25	−2.47	−2.47	−2.59	−1.26	0.86
PP_3	3.52	6.38	1.38	4.90	2.86	5.00	1.48	1.15	−1.11	−2.09	−2.09	−2.21	−1.24	0.88
PP_4	3.24	6.18	1.61	4.85	2.94	4.57	1.33	1.20	−1.07	−1.86	−1.87	−1.99	−1.23	0.89
PP_5	3.05	6.07	1.69	4.74	3.02	4.38	1.33	1.31	−0.96	−1.78	−1.79	−1.90	−1.24	0.88
PP_6	2.97	6.00	1.76	4.72	3.03	4.24	1.28	1.33	−0.94	−1.71	−1.71	−1.83	−1.24	0.88
PP_7	2.91	5.93	1.78	4.69	3.02	4.15	1.24	1.36	−0.90	−1.68	−1.68	−1.80	−1.25	0.88
CAM-B3LYP														
PP_2	4.33	6.94	0.87	5.20	2.62	6.07	1.74	0.91	−1.38	−2.62	−2.57	−2.70	−1.22	0.88
PP_3	3.87	6.59	1.22	5.09	2.72	5.37	1.50	1.02	−1.27	−2.29	−2.24	−2.37	−1.20	0.90
PP_4	3.65	6.46	1.36	5.01	2.82	5.10	1.45	1.10	−1.19	−2.15	−2.10	−2.24	−1.20	0.91
PP_5	3.52	6.38	1.40	4.92	2.87	4.98	1.46	1.20	−1.10	−2.12	−2.07	−2.20	−1.19	0.90
PP_6	3.46	6.38	1.44	4.90	2.91	4.94	1.48	1.22	−1.08	−2.07	−2.02	−2.16	−1.20	0.90
PP_7	3.43	6.34	1.44	4.88	2.90	4.89	1.46	1.24	−1.06	−2.06	−2.01	−2.14	−1.20	0.89
MN15														
PP_2	4.19	6.93	0.92	5.12	2.74	6.01	1.82	1.08	−1.36	−2.56	−2.52	−2.50	−1.27	0.80
PP_3	3.70	6.57	1.31	5.01	2.86	5.26	1.55	1.18	−1.25	−2.18	−2.14	−2.12	−1.27	0.81
PP_4	3.45	6.41	1.50	4.95	2.96	4.91	1.46	1.24	−1.19	−1.98	−1.95	−1.93	−1.27	0.81
PP_5	3.32	6.31	1.56	4.89	2.99	4.75	1.43	1.31	−1.13	−1.93	−1.89	−1.87	−1.27	0.80
PP_6	3.23	6.26	1.61	4.83	3.03	4.65	1.42	1.36	−1.07	−1.88	−1.84	−1.82	−1.27	0.81
PP_7	3.14	6.25	1.63	4.77	3.11	4.62	1.48	1.42	−1.01	−1.85	−1.81	−1.79	−1.27	0.81

Table S7: The free energy of PP_n-H_2O for each non-equivalent carbon binding site, all values are given with respect to C_3. For comparison we include equivalent data at the PP_2-TEA interface.

B3LYP										
Oligomer model	C_1	C_2	C_3	C_4	C_5	C_6	C_7	C_8	C_9	C_{10}
PP_2-H_2O	0.01	0.15	0.00	0.27						
PP_3-H_2O	0.00	0.17	0.00	0.29	0.17	0.03				
PP_4-H_2O	0.00	0.17	0.00	0.30	0.15	0.03	0.02	0.18		
PP_5-H_2O	0.01	0.18	0.00	0.30	0.14	0.03	0.02	0.17	0.16	0.02
PP_2-TEA	0.01	0.14	0.00	0.27						
CAM-B3LYP										
PP_2-H_2O	0.00	0.12	0.00	0.24						
PP_3-H_2O	0.01	0.14	0.00	0.26	0.16	0.03				
PP_4-H_2O	0.01	0.14	0.00	0.27	0.15	0.03	0.02	0.16		
PP_5-H_2O	0.01	0.15	0.00	0.27	0.13	0.03	0.02	0.15	0.14	0.02
PP_2-TEA	0.00	0.11	0.00	0.23						

Table S8: The free energy difference of competing reactions, for each of the exchange-correlation functionals used in the presence of an H_2O and TEA dielectric continuum.

H_2O			
Reaction	B3LYP	CAM-B3LYP	MN15
TEA + $TEA^{\bullet+}$ → TEA-H^+ + $TEAR^{\bullet}$	−0.02	−0.07	0.07
TEA + $TEAR^+$ + H_2O → TEA-H^+ + MeCHO + DEA	−0.16	−0.16	0.00
TEA			
Reaction	B3LYP	CAM-B3LYP	MN15
TEA + $TEA^{\bullet+}$ → TEA-H^+ + $TEAR^{\bullet}$	0.00	−0.05	−0.04
TEA + $TEAR^+$ + H_2O → TEA-H^+ + MeCHO + DEA	−0.12	−0.13	0.02

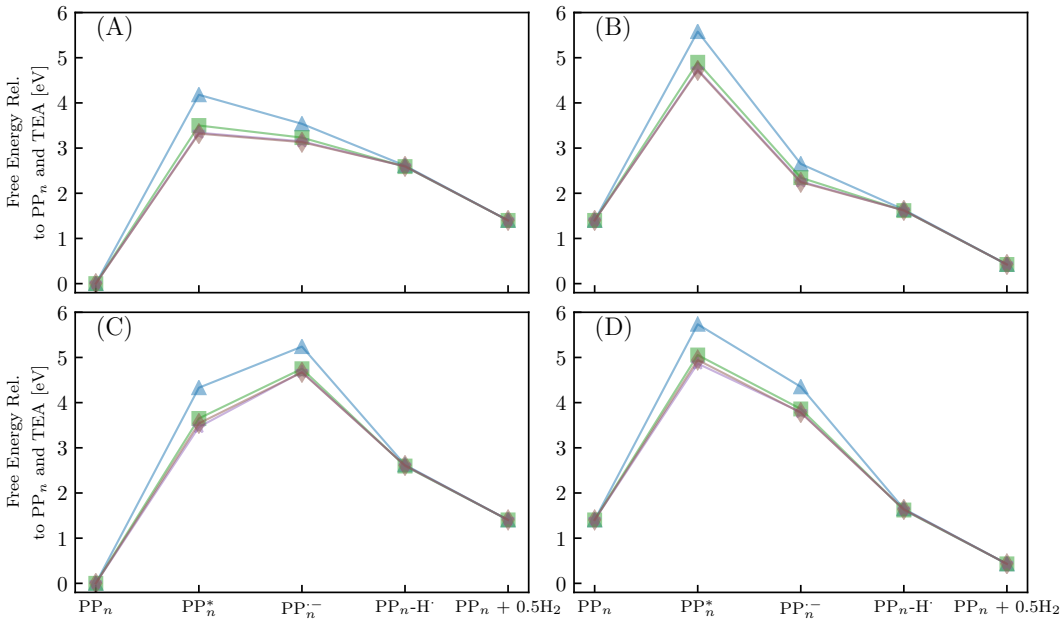

Figure S3: The predicted free energy profile for each step in H_2O of sub-cycle I (A) and II (B). The predicted free energy profile for each step in TEA of sub-cycle I (C) and II (D). Data shown for $n = 2$ (blue triangles), 4 (green squares), 6 (purple stars) and 7 (brown diamonds), calculated using CAM-B3LYP and provided relative to PP_n and TEA. The x-axis labels omit any reference to the SED or its degradation products.

References

(1) Fukuda, R.; Ehara, M. Electronic excited states and electronic spectra of biphenyl: A study using many-body wavefunction methods and density functional theories. *Physical Chemistry Chemical Physics* **2013**, *15*, 17426–17434.

(2) Lukeš, V.; Aquino, A. J. A.; Lischka, H.; Kauffmann, H. F. Dependence of optical properties of oligo-para-Phenylenes on torsional modes and chain length. *Journal of Physical Chemistry B* **2007**, *111*, 7954–7962.